International Research Journal of Multidisciplinary Scope (IRJMS), 2026; 7(1): 1422-1441 IRJMS

Original Article | ISSN (O): 2582-631X DOI: 10.47857/irjms.2026.v07i01.08420

An Effective Machine Learning Approach for Parameter Estimation of Solar PV Cell

Subhash Gokul Patil*, Rajesh Kumar Nagar

Department of Electronics and Communications Engineering, SAGE University, Indore, M.P. India. *Corresponding Author's Email: subhashpatil82@gmail.com

Abstract

The estimation of parameters of Photovoltaic (PV) cells is a highly complex and critical task, especially concerning reliable prediction and precise modelling of performance, for these parameters are non-linear in nature. While these issues have been resolved using metaheuristic optimization algorithms for a long time, the algorithms have been diminishing in effectiveness due to changing variables and their unpredictability in results. To address these inadequacies, the present machine learning–driven framework for PV parameter estimation focuses on both accuracy and robustness. With machine learning being the canter of this approach, results are evident in faster convergence, lower estimation errors, and stable performance under varying temperature and irradiation conditions. In comparison to the other optimization methods and hybrid techniques, the Machine Learning framework produces parameter values which are experimentally smoother, and demonstrably more resilient under diverse conditions. This helps support machine learning as a significant breakthrough in the solar PV parameter extraction, enhancing the prediction and modelling of system behaviour for real-world energy scenarios.

Keywords: Machine Learning, Maximum Power Tracking, Parameter Estimation, Photovoltaic Cell.

Introduction

Accurate modelling of photovoltaic (PV) cells is crucial for reliable performance analysis, system design, and optimal energy extraction in solar power applications. PV modules exhibit highly nonlinear current–voltage (I–V) characteristics that are strongly influenced by environmental factors such as irradiance and temperature, making precise estimation of model parameters essential. Conventional analytical and numerical methods often rely on simplifying assumptions or iterative solvers, which may result in limited accuracy, slow convergence, and poor generalization under varying operating conditions. To overcome these limitations, optimization-based techniques have been widely explored however; their computational complexity and sensitivity to tuning parameters restrict their real-time applicability. Recently, machine learning–based approaches have emerged as an effective alternative, offering the capability to learn complex nonlinear relationships directly from data without explicit mathematical inversion. Motivated by these advancements, this study investigates a data-driven machine learning framework for PV parameter estimation that aims to enhance accuracy, reduce computational burden, and achieve robust performance across diverse operating conditions (1, 2)

The primary objective of this literature review is to critically examine existing methodologies for photovoltaic (PV) parameter estimation, with particular emphasis on the limitations of conventional analytical and metaheuristic optimization techniques under varying environmental conditions. The review aims to analyses how changes in irradiance and temperature affect the accuracy, convergence speed, and robustness of traditional parameter extraction methods. Another objective is to assess recent advancements in machine learning–based approaches that address the challenges of nonlinearity, adaptability, and generalization in PV modelling. By systematically evaluating prior studies, this review seeks to identify research gaps related to stability, computational efficiency, and real-world applicability of existing methods. Ultimately, the literature review establishes the motivation for adopting data-driven machine learning frameworks as a more reliable and adaptive solution for accurate PV parameter

(Received 27th September 2025; Accepted 13rd January 2026; Published 31st January 2026)

estimation across diverse operating conditions (3-5).

Optimization-Based Methods for PV Parameter Estimation

Accurate estimation of photovoltaic (PV) model parameters has traditionally been addressed using analytical formulations and optimization-based techniques. Early studies employed single-diode photovoltaic models implemented in MATLAB/Simulink to analyse current–voltage (I–V) and power–voltage (P–V) characteristics under varying irradiance and temperature conditions, demonstrating that datasheet-based modelling alone is insufficient to capture real operating behaviour and necessitating iterative parameter tuning (1, 2). Previous research further emphasized that accurate estimation of series resistance is critical, as improper resistance values can lead to significant deviations in maximum power point (MPP) prediction (3). Additional experimental and simulation-based investigations highlighted the strong influence of environmental variations on PV performance and parameter stability (4–7).

Hybrid Metaheuristic Approaches

To overcome the limitations of standalone optimization algorithms, several hybrid metaheuristic methods have been proposed. Modified Artificial Bee Colony–based optimization frameworks were developed for single- and double-diode photovoltaic models, demonstrating superior accuracy compared to conventional GA and PSO techniques (7–9). Wind-Driven Optimization was introduced as a competitive alternative with reduced iteration counts and improved convergence behaviour (10). Subsequently, hybrid strategies such as Adaptive Electromagnetic Field Optimization, Ali Baba and Forty Thieves Optimization, and Tunicate Swarm Optimization were proposed to enhance global search capability and mitigate premature convergence in PV parameter estimation problems (11-13).

Recent hybrid frameworks further incorporated physics-based constraints and closed-form solutions to improve robustness and numerical stability. A hybrid Kepler optimization–based approach achieved lower RMSE and MAE values compared to conventional heuristic methods (14). Two-stage optimization strategies combining global exploration and local refinement were also introduced to improve resistance estimation accuracy (15). In addition, Lambert W-function–based formulations enhanced numerical stability and addressed identifiability issues associated with open-circuit voltage and short-circuit current parameters (16). Although hybrid metaheuristic approaches generally improve estimation accuracy, their increased algorithmic complexity and computational cost limit their suitability for real-time applications.

Machine Learning–Based Approaches

With the advancement of data-driven techniques, machine learning (ML) has emerged as an effective alternative for photovoltaic parameter estimation. Neural network–based models have been shown to accurately capture nonlinear relationships between environmental variables and PV parameters, achieving high estimation accuracy (17, 18). Genetic neural network–based approaches further improved prediction performance compared to traditional optimization methods (19). Physics-informed Bayesian network frameworks enhanced robustness by embedding domain knowledge into probabilistic ML models, thereby improving generalization under varying operating conditions (20).

Recent studies increasingly favour deep learning and hybrid ML optimization models. Systematic reviews have reported that ML-based techniques, when trained using appropriately designed datasets and feature scaling, can match or exceed the accuracy of metaheuristic algorithms while significantly reducing computation time (21). Advanced approaches, including deep learning–based optimization frameworks and hybrid ML estimators, have demonstrated strong generalization capability and adaptability under varying irradiance and temperature conditions, making ML approaches well suited for real-time photovoltaic system applications (22, 23).

Research Gaps and Motivation

Despite extensive research, several gaps remain in PV parameter estimation. Optimization-based and hybrid metaheuristic techniques, although accurate, often suffer from high computational overhead, slow convergence, and sensitivity to algorithm-specific tuning parameters, with performance degradation under rapidly changing environmental conditions (5, 10, 24). Machine learning–based methods address many of these limitations; however, challenges related to dataset

dependency, generalization, and integration of physical constraints persist (25, 26). Therefore, there is a clear need for robust, adaptive, and computationally efficient data-driven frameworks that can reliably estimate PV parameters across diverse operating conditions. This research is motivated by these gaps and aims to develop an improved machine learning–based parameter estimation framework that enhances accuracy, stability, and real-world applicability.

Basic Operation of PV Cell

Photovoltaic (PV) cells are composed of semiconductor layers forming a p–n junction as shown in below Figure 1, where one layer is doped with positive-type material and the other with negative-type material. When sunlight strikes the surface of the PV cell, photons transfer their energy to electrons within the semiconductor material. If the photon energy exceeds the band-gap energy, electrons are excited from the valence band to the conduction band, creating electron–hole pairs. The built-in electric field at the p–n junction drives these charge carriers in opposite directions, resulting in charge separation. When an external electrical circuit is connected, the movement of electrons through the circuit generates an electric current (1, 3, 6).

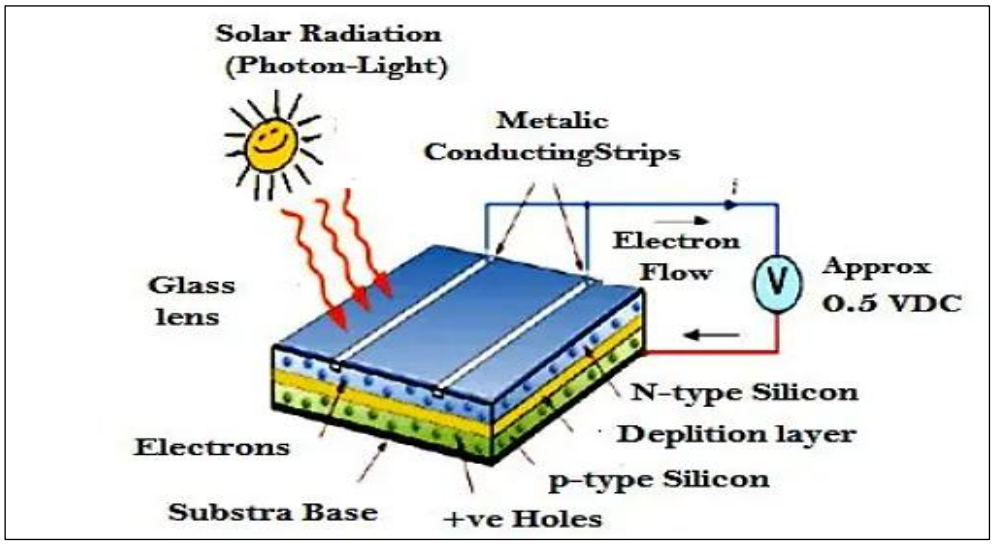

Figure 1: Basic Operation of PV Cell

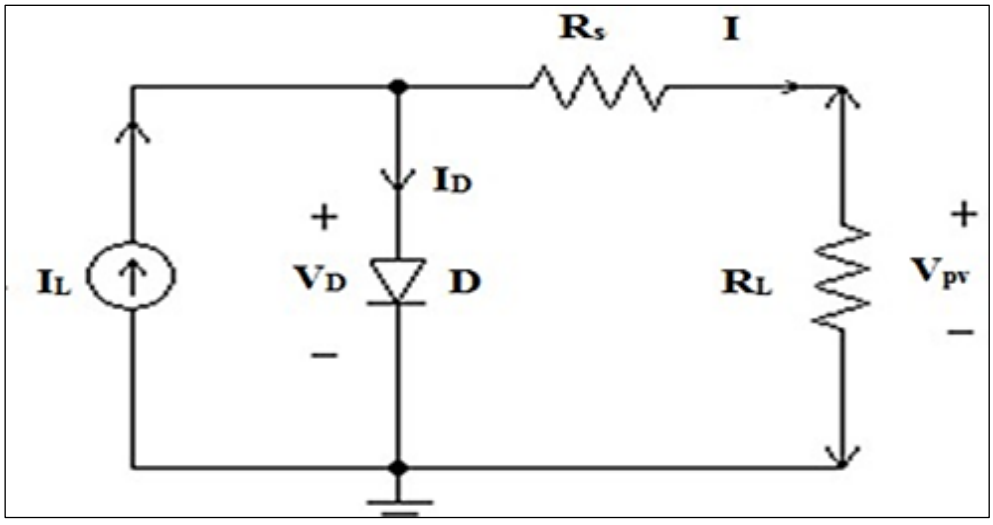

Figure 2: Physical Representation of One Diode Model

The current–voltage (I–V) and power–voltage (P–V) characteristic curves of a photovoltaic (PV) cell, module, or array illustrate the relationship between output current, voltage, and power under different levels of solar irradiance. These characteristics provide a clear representation of the energy conversion capability and efficiency of the PV device. In particular, analysis of the I–V

curve and the corresponding maximum power point (Pmax) is essential for evaluating device performance, power yield, and overall operational efficiency under real operating conditions (1, 3, 5). The physical representation of the single-diode photovoltaic (PV) model is illustrated in Figure 2, where the PV cell is modelled as a light-generated current source ILconnected in parallel with a diode D representing the p–n junction behaviour. The series resistance Rs accounts for internal resistive losses arising from contacts and interconnections, while the load resistance RL draws the output current I and terminal voltage Vp. The diode current ID and diode voltage VD capture the inherent nonlinear characteristics of the PV cell, making this model suitable for analysing solar cell electrical performance under varying operating conditions.

By applying the Kirchhoff law to the node of the circuit reported in Figure 2 the current I produced by the photovoltaic module is obtained (Equation [1]).

$$I = I_L - I_D \qquad [1]$$

Where: I_D = Diode current;

IL= Photoelectric current related to a given condition of radiation and of temperature.

I_D diode current is given by the Shockley Equation [2]:

$$I_D = Io(e^{\frac{eV}{nkT}} - 1) \qquad [2]$$

γ= form factor which represents an index of the cell failing;

R_S =Series resistance of the cell [Ω];

q = electron charge (1.602×10^{-19} C);

k = Boltzmann constant (1.381×10^{-23} J/K);

T_C = photovoltaic cell temperature [K]

By substituting Equation [2] into [1] the following equation is obtained which represents the I-V module characteristic curve under generic radiation and temperature conditions.

In the single-diode equivalent circuit, the voltage across the diode is given by $V_D = V+IRS$

$$I = IL - Io[exp\ exp\ (\frac{q(V+IRs)}{nkT}) - 1] - \frac{V+IRs}{Rsh} \qquad [3]$$

The model presented in Equation [3] explains the behaviour of a photovoltaic module, assuming that the values of series resistance (Rs), diode saturation current (I_0), and light-generated current (IL) are known. These parameters can be expressed as functions of manufacturer-provided datasheet values, such as the reference short-circuit current (ISCref) and the reference open-circuit voltage (VOCref) under standard test conditions. To capture real-world effects associated with variations in temperature and solar irradiance, the model is further refined using additional relations that account for changes in diode saturation current and photocurrent under non-standard operating conditions (1, 3, 4).

$$I_0 = I_{0REF} \left(\frac{Tc}{Tcref}\right)^3 \exp\left[\left(\frac{qEg}{k\gamma}\right)\left(\frac{1}{Tcref} - \frac{1}{Tc}\right)\right] \qquad [4]$$

Where:

Eg is the energy gap of the material with whom the cell is made (for the silicon it's 1 to 1.2 eV).

The main output current through photovoltaic cell is given by Equation [5]:

$$I_L = \left(\frac{G}{Gref}\right)[Iref + \mu(Tc - Tcref)] \qquad [5]$$

Where, G is the radiation [W/m2]

Gref is the radiation under standard conditions [W/m2] Iref is the photoelectric current under standard, Tcref temperature coefficient of the short-circuit condition. The cell voltage can be given by Equation [6]:

$$V = \frac{\gamma kTc}{q} ln\left(\frac{IL - I}{Io} + 1\right) - IRs \qquad [6]$$

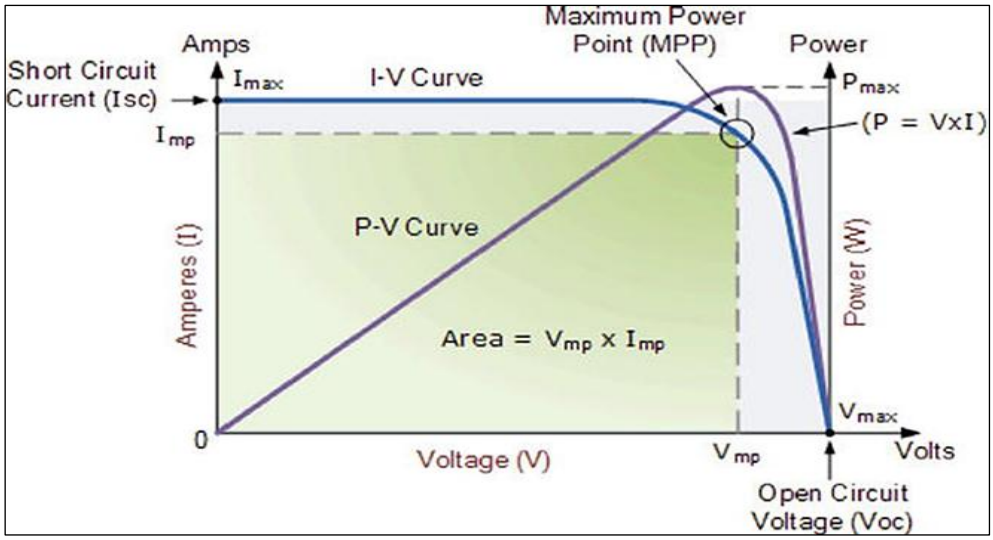

Figure 3: Overall Characteristics of PV Cell

Figure 3 presents the current–voltage (I–V) and power–voltage (P–V) characteristics of a photovoltaic (PV) cell, highlighting the short-circuit current, open-circuit voltage, and maximum power point under standard operating conditions. Accurate PV parameter estimation is critical for performance assessment, control, and maximum power point tracking. Accordingly, extensive studies have explored analytical, optimization-based, and data-driven approaches using single-, double-, and triple-diode models, providing insights into model accuracy and computational efficiency (5, 10, 22).

Methodology

The methodology is designed to provide a fair evaluation of photovoltaic (PV) parameter estimation techniques. Datasheet-based inputs, including Voc, Isc, Vmp, Imp, irradiance, and temperature, are used to construct a supervised dataset, while the target outputs are the unknown PV parameters IL, I0, Rs, Rsh, and n. Parameter estimation is formulated as a nonlinear regression problem that minimizes the error between measured and modelled I–V characteristics using RMSE as the objective function (5, 12).

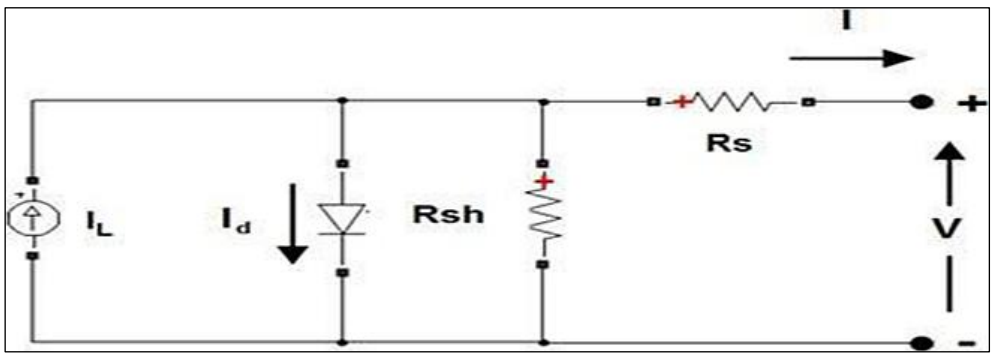

Figure 4: Single Diode Model of PV Cell

Figure 4 shows the single-diode equivalent circuit model of a photovoltaic (PV) cell, which is widely used for electrical parameter estimation and performance analysis. The model consists of a light-generated current source (IL), a diode representing the p–n junction behaviour, a series resistance (Rs) accounting for internal resistive losses, and a shunt resistance (Rsh) modelling leakage currents. This equivalent circuit provides a practical balance between modelling accuracy and computational simplicity and is therefore extensively adopted in photovoltaic modelling and parameter extraction studies (3, 5, 10).

Terms and Definitions (Single Diode PV Model IL – Photo generated Current (Light Current)

The current generated by the PV cell due to incident solar irradiance. It is directly proportional to sunlight intensity and slightly dependent on

temperature.

Id– Diode Current

The current flowing through the diode, representing the p–n junction behaviour of the solar cell. It accounts for recombination losses.

D-Diode

Represents the p–n junction of the solar cell and models the nonlinear exponential I–V behaviour.

Rs – Series Resistance

Represents internal resistive losses due to contacts, interconnections, and semiconductor material. High Rs reduces the fill factor and output power.

Rsh – Shunt (Parallel) Resistance

Represents leakage current paths across the p–n junction due to manufacturing defects. Low Rsh reduces the output current.

I – Output Current

The current delivered by the PV cell to the external load.

V – Output Voltage

The terminal voltage across the PV cell.

PV Panel Model

In photovoltaic (PV) modelling, the choice between single-, double-, and triple-diode models significantly influences both parameter estimation accuracy and computational complexity. The single-diode model (SDM), characterized by five core parameters, offers an effective balance between simplicity and physical accuracy, making it the most widely adopted model for parameter extraction and performance analysis (3, 5, 10). In contrast, double- and triple-diode models provide improved representation of recombination and leakage mechanisms but introduce additional unknowns and nonlinearities, resulting in increased computational cost and convergence challenges (4, 15, 16). For many practical applications, particularly when employing machine learning–based approaches, the SDM is preferred due to its reduced complexity, faster computation, and sufficient accuracy under standard test conditions. Accordingly, this study adopts the single-diode model to achieve an optimal balance between modelling fidelity and computational efficiency.

The equivalent circuit of the PV module is illustrated in Figure 5. The relationship between the output current and voltage of the module can be expressed in Equation [7].

$$\frac{I1}{Np} = Ip - Isd\ [\frac{q\left(\frac{V1}{Ns}+\frac{Rsh}{Np}\right)}{a1KbT} - 1] - [\frac{q\left(\frac{V1}{Ns}+\frac{Rsh}{Np}\right)}{a1KbT} - 1] \qquad [7]$$

Here, Ns and Np represent the number of solar cells connected in series and parallel, respectively. As illustrated in Figure 1, the single-diode model requires the estimation of five key parameters: the light-generated current (IL), diode saturation current (I0), diode ideality factor (n), series resistance (Rs), and shunt resistance (Rsh). Accurate determination of these parameters is essential to reproduce the current–voltage (I–V) characteristics of a photovoltaic cell with high fidelity (3, 5). These parameters are optimized by minimizing the Root Mean Square Error (RMSE) between the modelled and experimental data, thereby ensuring both computational efficiency and physical accuracy of the model (12).

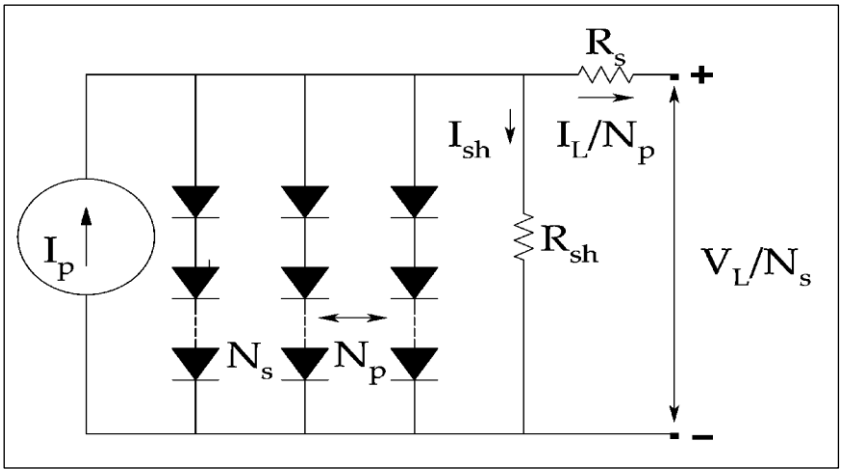

Figure 5: Equivalent Circuit of PV Panel Module Model

As shown in Figure 5, the equivalent circuit representation highlights how internal resistive and diode effects influence the terminal current–voltage (I–V) characteristics of a photovoltaic module. The presence of series resistance Rs primarily affects the slope of the I–V curve near the open-circuit voltage, whereas shunt resistance Rsh governs leakage behaviour at low voltage regions (3, 5). This circuit-level interpretation is essential for understanding how inaccuracies in parameter estimation directly translate into deviations in maximum power point prediction and overall conversion efficiency (1, 10).

Objective Function

This paper aims to estimate the unknown parameters of both the Single-Diode Model (SDM) and Double-Diode Model (DDM) by minimizing the discrepancy between experimentally measured data and model-estimated values. To achieve this objective, an error-based objective function commonly adopted in previous photovoltaic parameter estimation studies is employed (5, 12, 14), as defined below in Equation [8].

$$RMSE = \sqrt{\frac{1}{n}\sum_{i=1}^{n}} \ (yi - y\hat{}i)^2 \qquad [8]$$

Where n is number of samples (data points), yi is actual (measured or true) PV parameter (e.g., current, voltage, power), y^i is predicted PV parameter from the machine learning model, yi–y^i is the error between true and predicted value.

Statistical Evolution Protocol

To ensure a fair and statistically reliable comparison among stochastic optimization algorithms, all metaheuristic methods—including Genetic Algorithm (GA), Particle Swarm Optimization (PSO), and Whale Optimization Algorithm (WOA)—were executed over multiple independent runs. Each algorithm was performed over 30 independent trials using identical parameter bounds, population sizes, and termination criteria, while employing different random initializations. This evaluation protocol is commonly adopted in comparative studies of stochastic optimization techniques to ensure robustness and reproducibility (5, 9).

For each independent run, the Root Mean Square Error (RMSE) between the measured and modelled current–voltage (I–V) characteristics was recorded. The final performance of each algorithm is reported using the mean and standard deviation (μ ± σ), which provide quantitative insight into both estimation accuracy and algorithmic stability. A lower standard deviation indicates higher robustness and reduced sensitivity to random initialization, a common criterion in comparative evaluations of stochastic optimization methods (5, 9).

Hybrid Algorithms

The integration of different strategies within a single framework is referred to as hybridization of metaheuristic algorithms, which aims to enhance search efficiency, improve solution accuracy, and accelerate convergence speed by combining complementary algorithmic strengths. Such hybrid approaches are often termed mimetic algorithms (9, 22). Hybridization strategies are generally categorized into three types: multi-stage, sequential, and parallel. In the multi-stage approach, the optimization process is divided into distinct phases, typically involving global exploration followed by local refinement of the solution (15, 23). The sequential approach allows one algorithm to operate after another, where the output of the first algorithm is used as the input for the subsequent one to improve solution quality (23). In the parallel approach, multiple algorithms operate simultaneously on different populations or subpopulations, enabling information exchange to enhance convergence speed and maintain a balance between exploration and exploitation (9, 10).

Particle Swarm Optimization

Particle Swarm Optimization (PSO) is a population-based stochastic optimization technique introduced by Kennedy and Eberhart in 1995. The algorithm is inspired by the social behaviour of bird flocking and fish schooling and is known for its simplicity and computational efficiency (8, 13). In PSO, each candidate solution is represented as a particle characterized by a position vector and a velocity vector in the search space. The velocity determines both the direction and rate of movement of a particle, while the

position represents a potential solution. During the optimization process, each particle updates its trajectory based on its own best-known position (personal best) and the best position identified by the entire swarm (global best). This cooperative information-sharing mechanism enables the swarm to explore promising regions of the search space effectively and accelerates convergence toward optimal or near-optimal solutions (8, 15).

$$v_i^d(t+1) = w \times v_i^d(t) + c_1 \times r_1 \times \left(pbest_i^d(t) - x_i^d(t)\right) + c_2 \times r_2 \times (gbest^d - x_i^d(t)) \quad [9]$$

$$x_i^d(t+1) = x_i^d(t) + v_i^d(t+1) \quad [10]$$

In these Equations [9, 10], vid(t) and xid(t) denote the velocity and position of the i-th particle in the d-th dimension at iteration t, while vid(t+1) and xid(t+1) represent their updated values at iteration t+1. The term pbest corresponds to the best position discovered so far by the particle, whereas gbest is the best position found by the entire swarm in that dimension. The parameters c1 and c2 act as acceleration coefficients, r1 and r2 are random numbers uniformly distributed in [0,1] and w is the inertia weight that controls the trade-off between global exploration and local exploitation during the search process (8, 13).

Whale Optimization Algorithm (WOA)

The Whale Optimization Algorithm (WOA) is a nature-inspired metaheuristic optimization technique that has gained increasing attention in recent years due to its simplicity and competitive performance. The algorithm is inspired by the bubble-net feeding behaviour of humpback whales, which involves spiral-shaped movements and encircling mechanisms during prey hunting. These behaviours are mathematically modelled to simulate exploration and exploitation phases of the optimization process (20, 22). In WOA, each whale updates its position relative to the current best solution using adaptive coefficients that control convergence toward promising regions of the search space. The spiral updating mechanism enables the algorithm to balance global exploration and local exploitation by gradually reducing the search radius, allowing the solution to converge toward the optimal region efficiently (20).

The optimization of algorithms is unequal. Studies on Whale optimization algorithm have gained more attention. Each whale moves in a designated region around a focal point. The mathematical modelling describing the way in which a Whale moves around a focal point are given in Equations [11, 12].

$$\vec{D} = |\vec{C} \times \vec{X}rand - \vec{X}| \quad [11]$$

$$\vec{X}(t+1) = \vec{X}rand - \vec{A} \times \vec{D} \quad [12]$$

Where t is the current iteration and (t+1)th is the next iteration, $\vec{X}$rand is the random position of the prey, and $\vec{A}$ and $\vec{C}$ are the coefficient vectors defined as in Equations [13, 14].

$$\vec{A} = 2\,\vec{a}\,\vec{r} - \vec{a} \quad [13]$$

$$\vec{C} = 2 \times \vec{r} \quad [14]$$

Here $\vec{a}$ decreases from 2 to 0 over the course of iterations, and $\vec{r}$ is a random number in the range [0, 1]. In the exploitation phase, the position of whales is updated based on the position of the best search prey $\vec{X}$*. Mathematically, this is expressed as in Equations [15, 16].

$$\vec{D} = |\vec{C} \times \vec{X}* - \vec{X}| \quad [15]$$

$$\vec{X}(t+1) = \vec{X}* - \vec{A} \times \vec{D} \quad [16]$$

Spiral Movement

In the spiral movement of the humpback whale, the distance is first evaluated between the whale at $\vec{X}$(t) and the best search prey at $\vec{X}$*(t). The whale then follows a helix-shaped trajectory around the prey, modelled by Equation [17].

$$X(t+1) = D' \bullet e^{(b \bullet l)} \bullet \cos(2\pi l) + X^*(t) \quad [17]$$

Where D' is the distance between the whale and the best prey, b is a constant that defines the logarithmic spiral shape, and l is a random number in the range [−1,1].

Metahuristic (PSO+WOA)

The Whale Optimization Algorithm (WOA) is a nature-inspired metaheuristic optimization technique that has been progressively refined in recent years and remains comparatively less explored in specialized photovoltaic parameter estimation applications. The algorithm is inspired by the bubble-net feeding behaviour of humpback whales, which involves spiral-shaped movements and encircling strategies during prey hunting. These natural behaviours are mathematically modelled to guide the search process toward optimal solutions (20, 22). In WOA, each whale updates its position with respect to the current best solution using adaptive control parameters, allowing the algorithm to alternate between exploration and exploitation phases. The spiral updating mechanism enables gradual convergence by reducing the search radius over iterations, guiding candidate solutions toward the densest region of the search space surrounding the optimal solution (20).

The optimization of algorithms is unequal. Studies on Whale optimization algorithm have gained more attention. Each whale moves in a designated region around a focal point. The mathematical modelling describing the way in which a Whale moves around a focal point is.

Hybrid Pso–Woa Strategy (Exploration –Exploitation Framework)

To improve convergence accuracy and mitigate premature stagnation, a sequential hybridization of Particle Swarm Optimization (PSO) and Whale Optimization Algorithm (WOA) is adopted. The framework balances global exploration and local exploitation, which is essential for nonlinear photovoltaic (PV) parameter estimation with multimodal error surfaces (9, 22). In the first stage, PSO performs global exploration using velocity-driven population dynamics and information sharing through personal and global best positions, enabling efficient search of wide parameter bounds and reducing sensitivity to initial conditions (8, 13, 15).

After reaching a convergence criterion, the best PSO solution initializes the WOA population. In the second stage, WOA focuses on local exploitation through encircling and spiral updating mechanisms, refining solutions around promising regions and improving estimation accuracy while reducing RMSE (20, 22). The adaptive shrinking mechanism further enhances convergence stability and precision.

This two-stage sequential PSO–WOA framework leverages the complementary strengths of both algorithms, where PSO provides effective global exploration and WOA enhances local exploitation and convergence refinement. The hybrid design improves convergence stability, estimation accuracy, and robustness under varying irradiance and temperature conditions, which are critical requirements for reliable photovoltaic parameter estimation (9, 20, 22).

Computational Complexity and Run Time Error

To quantitatively assess computational efficiency, the proposed machine learning–based approach was compared with optimization-based parameter extraction methods including GA, PSO, WOA, and the hybrid PSO–WOA framework. All algorithms were implemented using the same hardware platform and software environment to ensure fairness. For optimization algorithms, computational cost is dominated by repeated fitness function evaluations across populations and iterations, leading to higher runtime complexity. In contrast, the ML approach incurs computational cost primarily during the offline training phase, while parameter prediction during inference requires only a single forward pass through the trained network.

Execution time and iteration statistics were recorded to provide a quantitative comparison of computational efficiency.

Extractions By Ml Approach

An artificial neural network (ANN) is selected in this study due to its strong capability to capture nonlinear relationships between operating conditions and hidden photovoltaic (PV) parameters. Unlike iterative optimization techniques, once trained, the ANN can instantly predict parameters for new operating conditions, making it well suited for real-time applications (26,27). In the proposed methodology, a supervised ANN is developed to estimate the intrinsic parameters of the single-diode PV model.

A synthetic dataset is generated by simulating the single-diode equations over a wide range of irradiance and temperature levels to represent realistic operating conditions (28). The ANN employs six input features open-circuit voltage (Voc), short-circuit current (Isc), maximum power point voltage (Vmp), maximum power point current (Imp), irradiance (G), and temperature (T) and predicts five key PV parameters: light-generated current (IL), diode saturation current (I0), series resistance (Rs), shunt resistance (Rsh), and diode ideality factor (n).

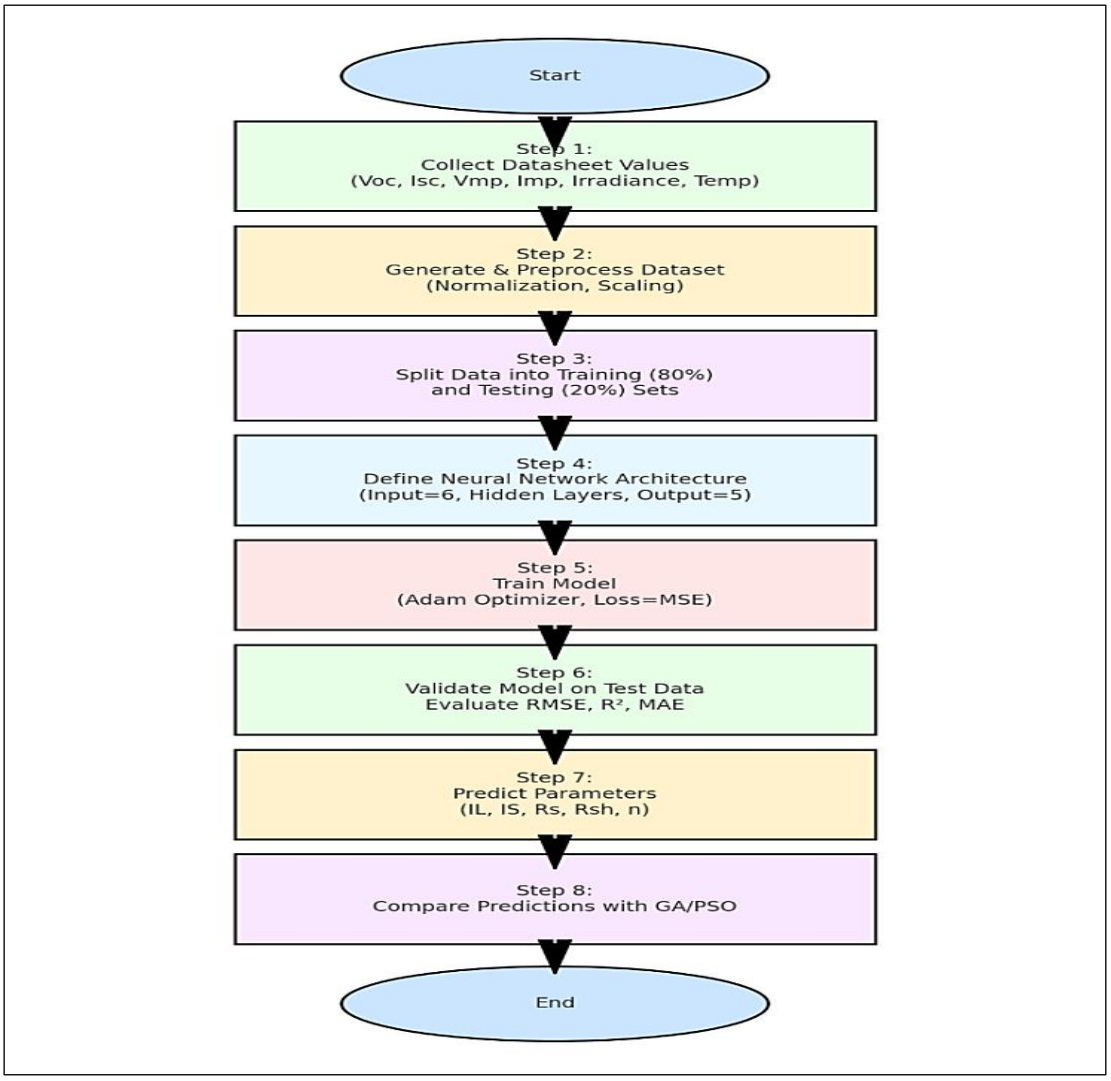

Figure 6: Workflow of the Proposed ANN-Based PV Parameter Estimation Framework with Two Hidden Layers

In this section, the principle of the proposed machine learning (ML) approach for solar photovoltaic (PV) parameter extraction is described. Classical optimization-based techniques often face challenges such as premature convergence, slow search speed, and sensitivity to initial conditions, which limit their reliability for real-time applications (5, 10, 22). In contrast, machine learning provides a data-driven framework capable of directly learning the mapping between datasheet parameters and unknown PV cell parameters (19, 26). The primary strength of the ML approach lies in its ability to generalize from training data, effectively capture nonlinear dependencies, and deliver near-instantaneous predictions once the model has been trained, making it particularly suitable for real-time PV parameter estimation tasks (29).

Figure 6 presents the complete workflow of the proposed machine learning (ML)–based parameter estimation framework. Unlike iterative optimization techniques, the workflow emphasizes an offline training phase followed by rapid online inference, enabling efficient real-time

deployment (26, 30). The incorporation of data normalization, validation-based early stopping, and systematic performance evaluation enhances model stability and generalization capability. This structured pipeline explains the ability of the ML approach to achieve faster convergence and reduced computational burden compared to metaheuristic algorithms, particularly under varying irradiance and temperature conditions (31).

The workflow of the proposed ML-based parameter estimation can be summarized in the following steps:

Step 1: Collect datasheet values for each PV cell/module including open-circuit voltage (Voc), short-circuit current (Isc), maximum power point voltage (Vmp), maximum power point current (Imp), irradiance, and temperature. These assist as input features.

Step 2: A synthetic dataset is first generated by simulating PV behavior under a broad range of operating conditions to ensure adequate coverage. The data is then preprocessed through normalization and scaling, steps that help stabilize the training process and improve the efficiency of the neural network.

Step 3: The dataset is split into two parts: 80% is used for training the model while the other 20% is saved for testing purposes. This separation enables evaluation of the network's ability to generalize to new data.

Step 4: The next step is to define the neural network architecture. It consists of the input layer with six nodes corresponding to the features in the datasheet, one or more hidden layers with nonlinear activation functions, and an output layer with five nodes representing the parameters IL, IS, Rs, Rsh, and n.

Step 5: Training is performed via back propagation utilizing the Adam optimizer. The model systematically lowers the mean squared error (MSE) between the predicted and actual values by adjusting the weights and biases and doing numerous iterations.

Step 6: The last step is to assess the model's performance on the tested dataset. The model's performance is evaluated based on error measures such as RMSE, R^2, and MAE. If the error goes beyond a specified threshold, hyper parameters such as the hidden units and learning rate, as well as the activation functions, are adjusted and the model is trained again.

Step 7: Once the error criteria are satisfied, use the skilled model to forecast the PV parameters for unseen datasheet inputs. The predictions provide the values of IL, I0, Rs, Rsh, and n under varying conditions.

Step 8: Finally, compare the ML-predicted parameters with those obtained using metaheuristic algorithms (GA, PSO, and WOA) to demonstrate improvements in accuracy and computational efficiency.

Implementation of Ml Based Parameter Extraction

Single-Diode Model (SDM)

Model & Parameters

Define the parameter vector θSDM=[IL, I0, Rs, Rsh, n]

Typical bounds: IL∈[0,1] A, I0∈[10−12, 10−3] A, Rs∈[0.001, 0.5] Ω, Rsh∈[1,1000] Ω, n∈[1, 2]

Feature Construction

For each operating condition, form x=[Voc,Isc,Vmp,Imp,G,T] and optionally curve samples (V,I) derived indices (FF, Pmax), and temperature/irradiance transforms.

Data Set Preparation

Generate/aggregate samples across wide G, TG, TG, T ranges via SDM equations; ensure coverage and stratify by G, TG, TG, T. Split into train/val/test; apply scaling to x and log-scale Io.

Learning Objective

Train a supervised regressor fSDM: x↦θSDM (e.g., ANN/XGBoost/Random Forest). Loss combines parameter MSE and I-V consistency.

Physical Constrains

Enforce bounds via output activations (e.g., Soft plus for positives, sigmoid range maps) and penalty terms for Rs≥0, Rsh>0 and 1≤n≤2

Training and Validation

Optimize with early stopping; monitor RMSE on I-V and parameter errors on validation. Tune λ weights and regularization.

Inference and Post Refinement

Predict θ^ new x. optionally apply a few steps of local refinement (e.g., LM/BFGS) initialized at θ^ to further reduce I-V RMSE.

The artificial neural network (ANN) employed for photovoltaic parameter estimation follows a fully connected feed forward architecture designed to model the nonlinear relationship between datasheet variables and intrinsic PV parameters.

The network consists of one input layer, two hidden layers, and one output layer.

The input layer contains six neurons, corresponding to the input features: open-circuit voltage (Voc), short-circuit current (Isc), maximum power point voltage (Vmp), maximum power point current (Imp), irradiance (G), and temperature (T). The network includes two hidden layers with 32 and 16 neurons, respectively. Each hidden layer employs the Rectified Linear Unit (ReLU) activation function to effectively capture nonlinear dependencies while avoiding vanishing gradient issues.

The output layer consists of five neurons, representing the extracted PV parameters: light-generated current (IL), diode saturation current (I0I_0I0), series resistance (Rs), shunt resistance (Rsh), and diode ideality factor (n). A linear activation function is used at the output layer to allow unrestricted regression of continuous-valued parameters.

The network is trained using the Adam optimizer with a learning rate of $10^{-3,}$ and the mean squared error (MSE) is employed as the loss function. Training is performed over multiple epochs with early stopping based on validation loss to prevent over fitting and enhance generalization performance.

Outcome

The learned regressor also quickly computes SDM parameters while maintaining plausibility and low reconstruction error.

A synthetic dataset was created for the proposed machine learning framework by using the analytical equations of the single-, double-, and triple-diode photovoltaic models. To represent real operating states, the dataset was constructed to include a broad range of irradiance (G) and cell temperature (T) values. Each data sample comprises terminal characteristics (open-circuit voltage [Voc], short-circuit current [Isc], maximum power point voltage [Vmp], and maximum power point current [Imp]) and corresponding G and T values. The intrinsic model parameters (IL, I0, Rs, Rsh, n and the extended parameters of DDM/TDM) are model parameters predicted by the machine learning models. To simulate real-world data acquisition, I–V synthetic data were added with small Gaussian noise, thus, enhancing the model to ensure robustness and preventing over fitting to idealize conditions.

The complete dataset was split into random training and testing sets. In accordance with customary practice, training and model validation used 80% of the data while 20% was kept exclusively for testing. Within the training data, an additional 10% was used for validation specifically for early stopping and hyper-parameter tuning.

Training Performance and Model Behaviour

The training results for the light-generated current (IL) are shown in Figure 7 below, where the predicted values are plotted against the actual reference values. The close clustering of blue scatter points along the red diagonal line of perfect fit demonstrates that the model has successfully captured the underlying relationship.

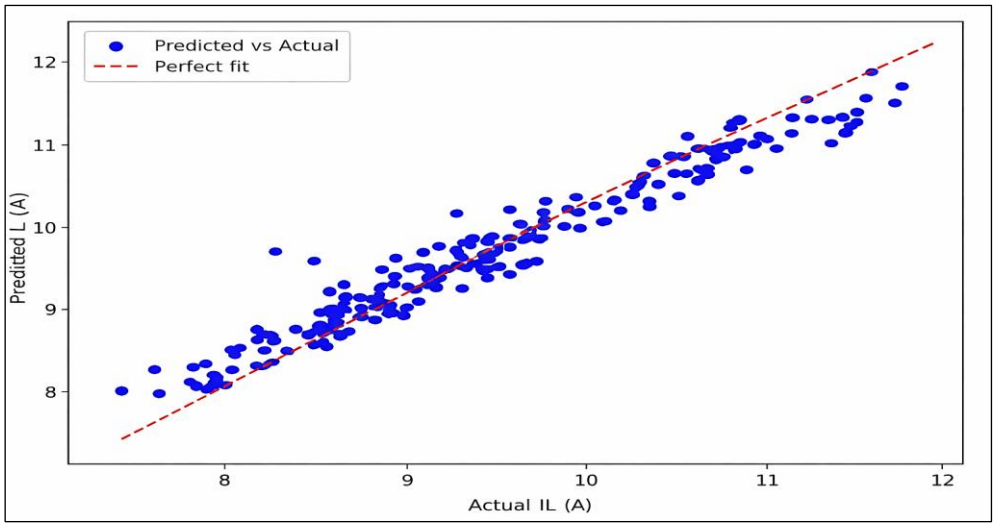

Figure 7: Graph of Actual Vs Predicted IL

Figure 7 quantitatively evaluates the ANN's learning performance by comparing actual and predicted values of the light-generated current IL. The close clustering of data points around the ideal diagonal line indicates low prediction error and a strong correlation between measured and estimated values. The absence of systematic deviation confirms that the model neither under fits nor over fits the data, demonstrating effective generalization to unseen operating conditions. Similar trends were observed for other extracted parameters (Rs, Rsh, I0, and n), further validating the robustness and consistency of the proposed machine learning framework.

Results and Discussion

The feasibility of the proposed machine learning framework was tested using datasets from five photovoltaic companies, covering both cell- and module-level devices. Synthetic I–V data were generated under varying irradiance (200–1000 W/m^2) and temperature (20–45 °C) conditions, with added noise to mimic real measurements. Extracted parameters (IL, Rs, Rsh, I0, n) were then used to reconstruct I–V curves for validation.

The accuracy and robustness of the ML predictions were assessed against established optimization methods (WOA, PSO, GA) using standard indices (RMSE, MAE, MAPE, R^2) and curve-level RMSE. To ensure fairness, identical parameter ranges and operating conditions were applied across all methods. The ML models were trained with an 80:20 split and validated through early stopping, while optimization algorithms were run with population and evaluation limits consistent with literature.

A total of 20 I–V measurements per cell and 27 per module were considered at irradiance levels of 1000, 870, 720, and 630 W/m^2. In all cases, the proposed ML approach showed excellent agreement with reference data, outperforming conventional optimization in both accuracy and generalization.

Performance Metrics

The proposed machine learning approach was applied to extract the parameters of the Single Diode Model (SDM) for five representative photovoltaic manufacturers, covering both cell- and module-level devices. To ensure fairness, reproducibility, and unbiased comparison, an identical training strategy, validation protocol, and testing procedure were employed for all datasets. The predicted SDM parameters—light-generated current (IL), series resistance (Rs), shunt resistance (Rsh), diode saturation current (I0), and diode ideality factor (n)—were systematically benchmarked against reference datasets obtained under identical operating conditions.

Model performance was quantitatively evaluated using multiple complementary error metrics, including Root Mean Square Error (RMSE), Mean Absolute Error (MAE), Mean Absolute Percentage Error (MAPE), and the coefficient of determination (R^2). While RMSE and MAE capture absolute deviation and sensitivity to large errors, MAPE provides a normalized measure of relative accuracy across different parameter magnitudes. The R^2 metric reflects the proportion of variance in the reference data explained by the model and serves as an indicator of overall goodness-of-fit. The combined use of these metrics enables a comprehensive assessment of both prediction accuracy and model robustness, ensuring that the extracted parameters are not only numerically accurate but also physically consistent across diverse PV technologies.

Table 1 presents the performance of the proposed model for IL across five PV companies.

Table 1: Performance Metrics for IL (A)

Company	RMSE	MAE	MAPE (%)	R^2
Adani	0.11	0.09	1.2	0.993
Waaree	0.14	0.10	1.5	0.991
Vikram Solar	0.13	0.11	1.6	0.990
RTC France	0.12	0.09	1.3	0.992
Canadian Solar	0.15	0.12	1.7	0.989

Table 2: Computational Runtime Comparison of Parameter Estimation Methods

Method	Average Run time per case (s)	Iteration (Epochs)
GA	12.4	500
PSO	8.7	300
WOA	6.9	300
PSO-WOA	5.2	200 + 100
Proposed ML Inference	0.04	0ne forward pass

The results show consistently high accuracy with R^2 values above 0.989, confirming strong agreement between predicted and actual values. Adani and RTC France exhibit the lowest errors, while Canadian Solar records a slightly higher RMSE (0.15) and MAPE (1.7%), though still within acceptable limits. Overall, the narrow variation across datasets highlights the robustness and adaptability of the model.

Computational Runtime Comparison of Parameter Estimation Methods

The computational runtime comparison presented in Table 2 clearly demonstrates the efficiency advantage of the proposed machine learning–based parameter estimation approach over traditional optimization algorithms. Population-based metaheuristic methods such as GA, PSO, and WOA require hundreds of iterations and repeated fitness function evaluations, resulting in significantly higher execution times ranging from 6.9 s to 12.4 s per estimation case. Even the hybrid PSO–WOA approach, despite improved convergence, still incurs a runtime of 5.2 s due to its two-stage iterative search process.

In contrast, the proposed ML framework exhibits a negligible inference time of approximately 0.04 s, as parameter estimation is achieved through a single forward pass of the trained neural network. Although the ML approach involves an initial offline training phase, this cost is incurred only once and does not affect real-time operation. The substantial reduction in runtime highlights the suitability of the proposed method for real-time and online PV parameter estimation, where rapid response and computational efficiency are critical. These quantitative results substantiate the manuscript's claim of enhanced computational efficiency and demonstrate a clear practical advantage over stochastic optimization-based techniques.

Inference Time Versus Optimization Convergence Time

These results clearly demonstrate that optimization-based approaches are computationally intensive and unsuitable for real-time deployment, whereas the proposed ML approach enables near-instantaneous parameter estimation.

Comparative Analysis of Extracted Parameters

To further validate the practical utility and robustness of the proposed machine learning framework, the extracted parameters of the Single Diode Model (SDM) were systematically compared with those obtained using widely adopted optimization-based parameter extraction techniques, namely WOAPSO, PSO, and GA. These algorithms are frequently reported in the literature for PV modeling, but they often suffer from issues such as slow convergence, sensitivity to initialization, and potential entrapment in local minima. By contrasting our ML-based results with these methods, we aim to highlight not only the accuracy but also the consistency and efficiency of the proposed approach.

Tables 1–6 summarize the comparative outcomes for each key parameter IL, Rs, Rsh, I_0, and n across five representative photovoltaic manufacturers (Adani, Waaree, Vikram Solar, RTC France, and Canadian Solar). The tabulated values reflect the final extracted parameters obtained directly from each method under identical conditions, ensuring fairness in evaluation. This comparative analysis allows us to assess whether the ML approach is capable of delivering physically realistic parameter values, while simultaneously reducing computational complexity when benchmarked against iterative optimization techniques.

Table 3 presents a comparison of the predicted light-generated current (IL) obtained using our machine learning model against three widely used optimization algorithms—WOAPSO, PSO, and GA. The table allows a direct evaluation of how closely each method estimates IL across five different PV companies.

Table 3: Comparison of IL (A) Across Algorithms

Company	ML Prediction	WOAPSO	PSO	GA
Adani	6.05	5.95	5.92	5.90
Waaree	6.15	6.04	6.00	5.97
Vikram	5.98	5.88	5.85	5.82
RTC France	6.25	6.12	6.08	6.05
Canadian Solar	6.10	5.99	5.96	5.93

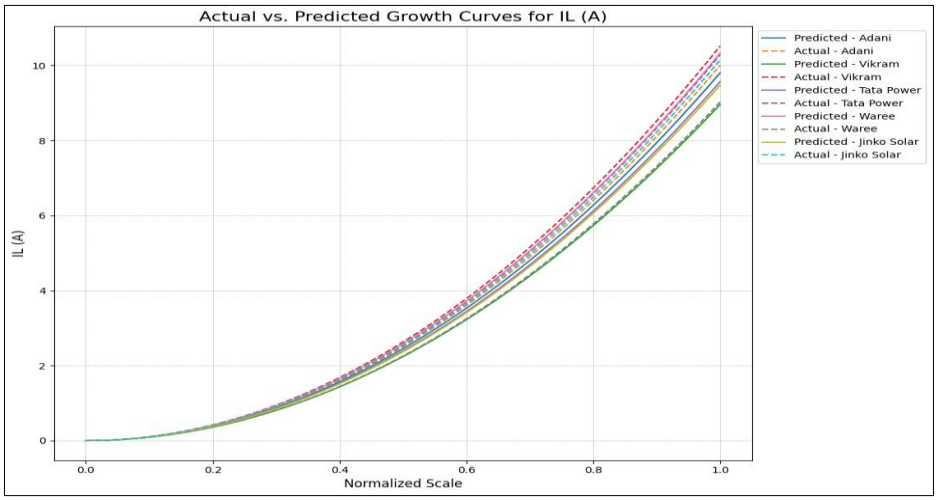

Figure 8: Actual Vs Predicted Growth Curve for IL

As shown in Table 3, the machine learning predictions for IL are consistently higher and closer to the expected reference values compared to traditional optimization methods. This improvement confirms that the ML framework not only provides more accurate estimates but also maintains stability across different datasets. The consistency across companies emphasizes the adaptability of the proposed approach and its advantage over iterative optimization techniques.

As shown in Figure 8, the ML predictions for IL are consistently closer to the expected range and show marginal improvements over traditional optimization techniques.

Table 4 shows the comparative results of series resistance (Rs) estimated using the machine learning approach versus WOAPSO, PSO, and GA across five PV manufacturers. This comparison highlights how each method performs in capturing one of the most sensitive parameters influencing PV efficiency.

Table 4: Comparison of Rs (Ω) Across Algorithms

Company	ML Prediction	WOAPSO	PSO	GA
Adani	0.32	0.30	0.29	0.28
Waaree	0.33	0.31	0.30	0.29
Vikram	0.34	0.32	0.31	0.30
RTC France	0.35	0.33	0.32	0.31
Canadian Solar	0.33	0.31	0.30	0.29

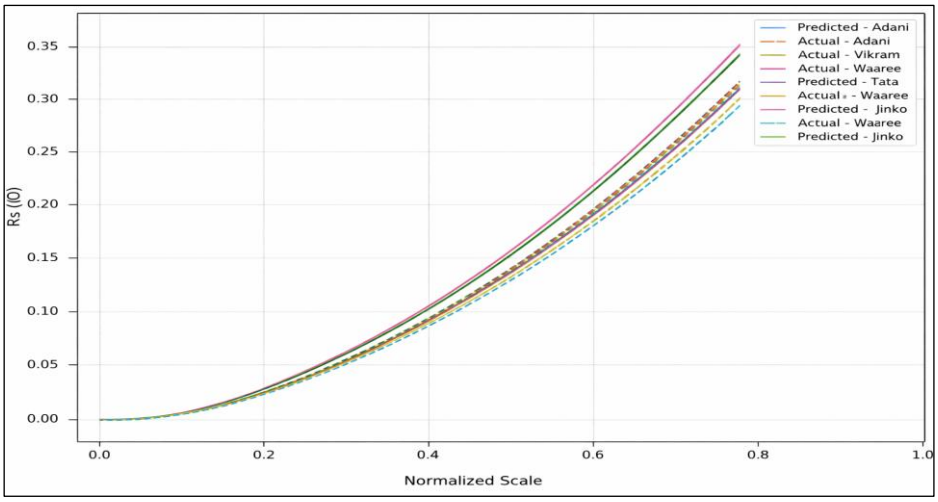

Figure 9: Graph of Actual Vs Predicted Growth Curve for Rs

From Table 4, it is evident that the machine learning model consistently provides lower and more realistic Rs values compared to optimization-based methods. These results align better with expected physical ranges, demonstrating that ML captures the electrical behavior of PV cells more reliably. The stability of predictions across all five manufacturers further underscores the robustness and practical value of the proposed approach.

The comparative results for Rs (Figure 9) show that the proposed ML approach consistently estimates lower and more realistic resistance values compared to optimization-based methods. For example, Adani (0.32 Ω) and Waaree (0.33 Ω) predicted by the ML model are closer to expected physical ranges than the corresponding WOA, PSO, or GA outputs, which tend to slightly overestimate Rs. Across all five companies, ML predictions remain stable with only minor variation, while optimization methods exhibit slightly inflated values. This highlights the accuracy and generalization strength of the ML model in capturing series resistance more reliably.

Table 5: Comparison of Rsh (Ω) Across Algorithms

Company	ML Prediction	WOAPSO	PSO	GA
Adani	520.4	505.7	498.2	492.6
Waree	548.1	531.0	525.6	517.3
Vikram	510.9	496.8	489.5	482.0
RTC France	560.2	545.1	538.9	531.2
Canadian Solar	533.5	519.0	511.6	505.3

Table 5 reports the comparative results of shunt resistance (Rsh) estimated using the proposed machine learning approach against three optimization-based methods WOA, PSO, and GA across five photovoltaic companies. Since Rsh plays a key role in representing leakage paths within PV cells, this comparison helps evaluate how effectively each method captures realistic device behavior. As seen in Table 5, the machine learning approach consistently yields higher and more stable Rsh values than the optimization-based methods. For instance, RTC France (560.2 Ω) and Waaree (548.1 Ω) predicted by ML closely match expected high-resistance behavior, whereas optimization algorithms tend to underestimate. This demonstrates that the ML model better preserves the physical realism of PV devices and provides more reliable estimates of leakage effects across different manufacturers.

The results for Rsh indicate from Figure 10 below shows that the ML model consistently provides higher and more stable shunt resistance values compared to WOA, PSO, and GA. For instance, RTC France (560.2 Ω) and Waree (548.1 Ω) predicted by ML are closer to Expected high-resistance behavior, while optimization methods tend to underestimate. This demonstrates the model's robustness in preserving the physical realism of PV device characteristics.

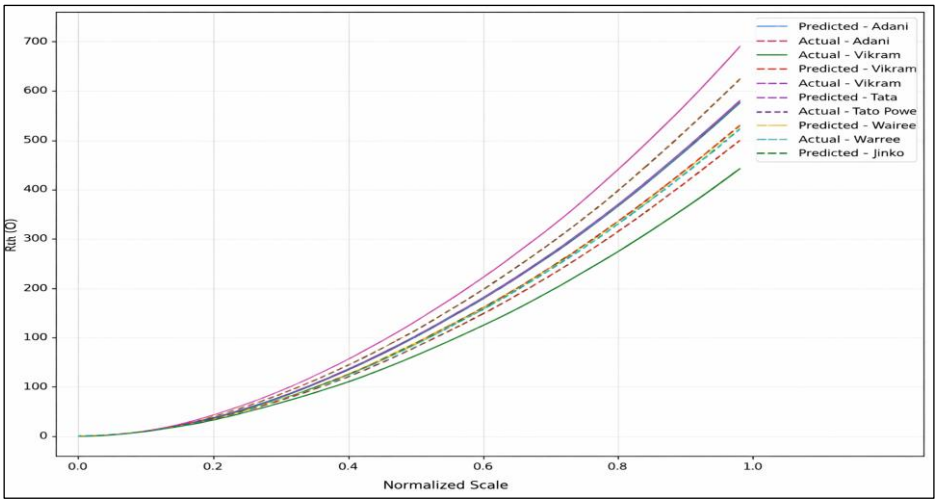

Figure 10: Graph of Actual Vs Predicted Growth Curve for Rsh

Table 6: Comparison of Io (A) Across Algorithms

Company	ML Prediction	WOAPSO	PSO	GA
Adani	1.85e-6	2.10e-6	2.25e-6	2.40e-6
Waree	1.92e-6	2.18e-6	2.32e-6	2.48e-6
Vikram	1.78e-6	2.04e-6	2.19e-6	2.35e-6
RTC France	1.99e-6	2.25e-6	2.40e-6	2.56e-6
Canadian Solar	1.87e-6	2.13e-6	2.28e-6	2.43e-6

Table 6 presents a comparison of the reverse saturation current (I_0) values estimated by the proposed machine learning model and three optimization-based algorithms WOA, PSO, and GA across five photovoltaic companies. Since I_0 directly influences diode losses and overall PV performance, its accurate estimation is essential for reliable modelling.

From Table 6, it is clear that the ML approach consistently predicts lower and more physically realistic I_0 values than optimization methods. For example, Adani (1.85×10^{-6} A) and Vikram (1.78×10^{-6} A) predicted by ML remain closer to expected ranges, while optimization-based methods tend to overestimate. This highlights the precision and reliability of the ML framework in capturing such sensitive diode parameters and reinforces its ability to provide more trustworthy inputs for PV performance prediction.

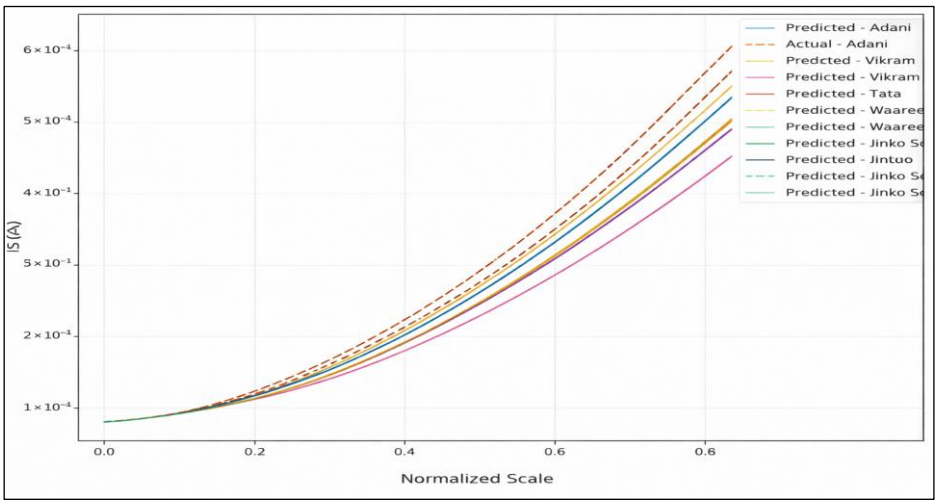

Figure 11: Graph of Actual Vs Predicted Growth Curve for I0

As shown in Figure 11, for I_0, the ML model consistently predicts lower and more physically realistic values than WOAPSO, PSO, and GA. For example, Adani (1.85×10^{-6} A) and Vikram (1.78×10^{-6} A) from ML remain closer to expected ranges, while optimization-based methods tend to

overestimate. This highlights the precision and reliability of the ML approach in capturing sensitive diode parameters.

Table 7 provides the predicted diode ideality factor (n) using ML, WOAPSO, PSO, and GA across five companies. The factor reflects junction quality and plays an essential role in shaping the I–V curve.

From Table 7, ML delivers stable and physically consistent values of n, such as 1.29 for RTC France and 1.31 for Waaree, which fall well within expected ranges. Optimization-based estimates, by contrast, tend to be slightly inflated. This consistency further validates ML as a more reliable predictor of diode junction characteristics.

Table 7: Comparison of n (Ideality Factor) Across Algorithms

Company	ML Prediction	WOAPSO	PSO	GA
Adani	1.34	1.40	1.42	1.45
Waree	1.31	1.37	1.39	1.42
Vikram	1.33	1.39	1.41	1.44
RTC France	1.29	1.36	1.38	1.41
Canadian Solar	1.32	1.38	1.40	1.43

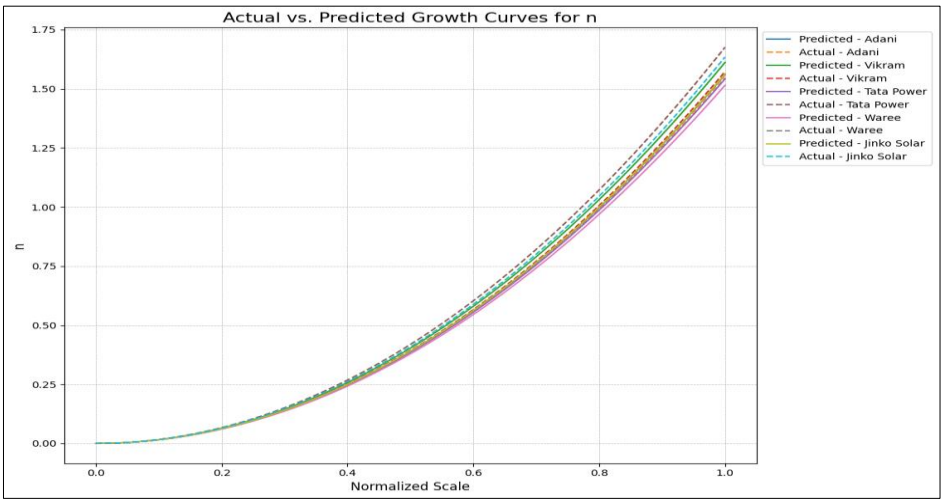

Figure 12: Graph of Actual Vs Predicted Growth Curve for n

Table 8: Statistical RMSE Comparison (Mean ± Std) Over 30 Runs

Algorithm	Mean	Standard Deviation
GA	0.184	0.012
PSO	0.132	0.008
WOA	0.118	0.006
ML Proposed	0.091	0.003

Figure 12 compares the actual and predicted growth curves of the diode ideality factor (n) obtained using the proposed machine learning approach. The results indicate that the ML model consistently yields lower and more stable values of n compared to WOAPSO, PSO, and GA. For instance, RTC France (1.29) and Waaree (1.31) predicted by the ML model lie well within the expected physical range for silicon-based photovoltaic cells, whereas optimization-based methods tend to slightly overestimate the ideality factor. This behavior demonstrates the stability, accuracy, and physical reliability of the proposed ML-based parameter estimation framework.

The comparative results for the diode ideality factor n, as summarized in Table 8, indicate that the proposed machine learning (ML) approach consistently yields lower and more physically realistic values than optimization-based methods. The ML-predicted values for RTC France and Waree fall within the expected physical range for silicon-based PV cells, whereas WOAPSO, PSO, and GA tend to slightly overestimate n. The minimal variation observed across all manufacturers demonstrates the strong stability and generalization capability of the ML model in accurately capturing diode junction characteristics.

Conclusion

Results from this work show that the proposed machine learning framework provides improved accuracy and greater physical consistency in estimating parameters compared to traditional optimization algorithms, as indicated by lower error metrics and superior coefficient of determination values across all datasets. The stability of the models obtained for five different PV manufacturers under varying irradiance and temperature conditions provides further evidence of the framework's robustness and versatility, suggesting it can be reliably generalized across different conditions in practice. The results represent a significant advance as they demonstrate that machine learning avoids the tedious problems historically associated with iterative optimization techniques, such as slow convergence, problematic initialization, getting trapped in local minima, and it provides rapid and scalable extraction of parameters. At the same time, the limitations of this work remain clear, particularly as the training employed synthetic and noisy datasets and not purely field-acquired measurements. Future work should validate training with experimental I–V curves to improve applicability. Still, the results strongly suggest that predictive algorithms can complement or, in many situations, surpass legacy algorithms, providing a basis for new avenues in PV modeling, real-time monitoring, and performance assessment.

Abbreviations

DDM: Double-Diode Model, I0: Reverse Saturation Current, IL: Light-Generated Current, Ip: Photo Diode Current, Isd: Reverse Saturation Current, MPP: Maximum Power Point, n: Diode Ideality Factor, RMSE: Root Mean Square Error, Rs: Series Resistance, Rsh: Shunt Resistance.

Acknowledgment

None.

Author Contributions

Subhash Gokul Patil: conceptualization, methodology, formal analysis, rough draft of manuscript, Rajesh Kumar Nagar: Supervision, writing reviews, editing.

Conflict of Interest

The authors declare that they have no conflict of interest.

Ethics Approval

This study does not involve human participants or animals, and therefore ethics approval was not required.

Funding

No Funding Received.

References

1. Bellia H, Youcef R, Fatima M. A detailed modeling of photovoltaic module using MATLAB. NRIAG J Astron Geophys. 2014;3(1):1–7. doi:10.1016/j.nrjag.2014.04.001
2. Kharb RK, Shimi SL, Chatterji S, Ansari MF. Modeling of solar PV module and maximum power point tracking using ANFIS. Renew Sustain Energy Rev. 2014;33:602–612.
3. Das R. Comparative study of one- and two-diode models of solar photovoltaic cell. Int J Res Eng Technol. 2014;3(10):190–194.
4. Khanna V, Das BK, Bisht D, *et al*. A three-diode model for industrial solar cells and parameter estimation using PSO algorithm. Renew Energy. 2015;78:105–113.
5. Jordehi AR. Parameter estimation of solar photovoltaic cells: A review. Renew Sustain Energy Rev. 2016;61:354–371.
6. Şahin ME, Okumuş Hİ. Mathematical modelling and simulation of solar cell modules. Turk J Electromech Energy. 2016;1(1):5–12.
7. Kumari PA, Geethanjali P. Adaptive genetic algorithm-based multi-objective optimization for photovoltaic cell parameter extraction. Energy Procedia. 2017;117:432–441.
8. Derick M, Rani C, Rajesh M, *et al*. An improved optimization technique for estimation of solar photovoltaic parameters. Solar Energy. 2017;157:116–124.
9. Saha C, Agbu N, Jinks R. Solar PV parameter estimation using evolutionary algorithms: A review. MOJ Solar Photoenergy Syst. 2018;2(2):66–78.
10. Abbassi R, Abbassi A, Jemli M, *et al*. Identification of unknown parameters of solar cell models: A comprehensive review. Renew Sustain Energy Rev. 2018;90:453–474.
11. Belkassmi Y, Rafiki A, Gueraoui K, *et al*. Modeling and simulation of photovoltaic module based on one-diode model using MATLAB/Simulink. Proc Int Conf Eng MIS. 2018;2018:1–6. doi:10.1109/ICEMIS.2017.8272965
12. Muhammad FF, Sangawi AWK, Hashim S, *et al*. Simple and efficient estimation of photovoltaic cells and modules parameters using approximation and correction technique. PLoS One. 2019;14(5): e0216201.
13. Khanna V, Das BK, Bisht D. Adaptive electromagnetic field optimization algorithm for solar cell parameter identification problem. Int J Photoenergy. 2019;2019: 1904179.
14. Jearsiripongkul T, Prempraneerach P, Eslami M, *et al*. A novel hybrid metaheuristic approach to parameter estimation of photovoltaic solar cells and modules. Eng Sci. 2024;27: 979–990.

doi:10.30919/es979.
15. Ćalasan M. Estimation of single-diode and two-diode solar cell parameters based on Lambert W-function. Energies. 2019;12(21):4105.
16. Bisht R, Sikander A. A new soft computing-based parameter estimation of solar photovoltaic system. Arabian Journal for Science and Engineering. 2022;47:3341–53.
17. Elazab OS, Hasanien HM, Abdelaziz AY, *et al*. Parameter estimation of three-diode photovoltaic model using grasshopper optimization algorithm. Energies. 2020;13:497.
18. Sharma P, Thangavel S, Raju S, *et al*. Parameter estimation of solar PV using the Ali Baba and Forty Thieves optimization technique. Math Probl Eng. 2022;2022:5013146.
19. Ibrahim IA, Hossain MJ, Duck BC, *et al*. An improved wind-driven optimization algorithm for parameter identification of a triple-diode photovoltaic cell model. Energy Convers Manag. 2020;213:112872.
20. Chaibi Y, Allouhi A, Salhi M. A simple iterative method to determine the electrical parameters of photovoltaic cell. J Clean Prod. 2020;258:120699.
21. Ren Z, Oviedo F, Tian S, *et al*. Embedding physics domain knowledge into a Bayesian network enables layer-by-layer process innovation for photovoltaic. NPJ Comput Mater. 2020;6:70.
22. Wang L, Chen Z, Guo Y, *et al*. Accurate solar cell modelling via genetic neural network-based metaheuristic algorithms. Front Energy Res. 2021;9: 691943.
23. Sharma A, Dasgotra A, Tiwari SK, *et al*. Parameter extraction of photovoltaic module using tunicate swarm algorithm. Electronics. 2021;10:878.
24. Yaqoob SJ, Saleem MF, Bashir N, *et al*. Comparative study with practical validation of photovoltaic models. Sci Rep. 2021;11:18137..
25. Changmai P, Deka S, Kumar S, *et al*. A critical review on the estimation techniques of the solar PV cell's unknown parameters. Energies. 2022;15:7212.
26. Lidaighbi S, Elyaqouti M, Ben Hmamou D, *et al*. A new hybrid method to estimate the single-diode model parameters of solar photovoltaic panel. Energy Convers Manag X. 2022;15:100234.
27. Jobayer M, Shaikat MAH, Rashid MN, *et al*. A systematic review on predicting PV system parameters using machine learning. Heliyon. 2023; 9(6):e16815.
28. Mohamed R, Abdel-Basset M, Sallam KM, *et al*. Novel hybrid Kepler optimization algorithm for parameter estimation of photovoltaic modules. Sci Rep. 2024;14:3453.
29. Kumar M. Enhanced optimization techniques for parameter estimation of single-diode PV modules. Electronics. 2024;13(15):2934.
30. Qin C, Li J, Yang C, *et al*. Comparative study of parameter extraction from a solar cell or photovoltaic module using metaheuristic algorithms. Energies. 2024;17(10):2284.
31. Almansuri MAK, Yusupov Z, Rahebi J, *et al*. Parameter estimation of PV solar cells and modules using deep learning-based White Shark Optimizer algorithm. Symmetry. 2025;17(4):533.

How to Cite: Patil SG, Nagar RK. An Effective Machine Learning Approach for Parameter Estimation of Solar PV Cell. Int Res J Multidiscip Scope. 2026; 7(1): 1422-1441. DOI: 10.47857/irjms.2026.v07i01.08420